# **RSC** Advances



View Article Online

View Journal | View Issue

PAPER



Cite this: RSC Adv., 2021, 11, 3870

# Transformation of alkali and alkaline earth metals during the preparation of activated carbon from Zhundong high-alkali coal

Dingcheng Liang, 💿 \* Qiang Xie, Jinchang Liu, Deqian Liu, Chaoran Wan and Shuai Yang

The preparation of activated carbon (AC) is a promising approach for the efficient utilization of Zhundong high-alkali coal. The volatilization and release of alkali and alkaline earth metal (AAEM) species can be effectively inhibited by using a lower operating temperature and a carbon matrix. However, the long time of the pyrolysis and activation process may promote the release of the AAEM from the coal during the process. Therefore, it is necessary to explore the transformation of AAEM during the preparation of AC from Zhundong high-alkali coal, and the cleanness of this process is evaluated accurately. In this study, the evolution of AAEM, distribution, and chemical speciation is characterized before and after the preparation of AC from the coal, and then thermodynamic calculations were performed using FactSage to simulate the transformation of AAEM in the coupled process of pyrolysis and activation. The results showed that in the process of AC preparation, the AAEM species inside the carbon matrix moved towards the surface of the AC with the aid of released volatiles and the activation reaction. Some Na and K species were released due to their weak binding with the carbon matrix and this resulted in the loss of Na and K content, whereas Mg and Ca were closely combined with the carbon matrix and were enriched in the AC. Furthermore, the defects and amorphous structure of the AC prepared with H<sub>2</sub>O activation were more than that of the AC prepared with CO2 activation, which meant that more of the AAEM species were exposed to the high temperature environment. As a result, the loss of AAEM content in the AC with  $H_2O$  activation was higher than that in the AC with  $CO_2$  activation. In this process, a small amount of highly volatile and corrosive AAEM was produced, and the release of volatile matter and the consumption of the carbon matrix were the main factors for the AAEM loss. Therefore, the preparation of AC from Zhundong high-alkali coal is a viable method for its clean use.

Received 9th November 2020 Accepted 7th January 2021

DOI: 10.1039/d0ra09518d rsc.li/rsc-advances

#### 1. Introduction

In China, the traditional activated carbon (AC) industries used to be concentrated in the Ningxia and Shanxi Provinces. Together with the continuous development of coal resources in the Xinjiang Uyghur Autonomous region, the AC industry gradually started moving to that region.<sup>1</sup> The Shenhua Xinjiang Energy Co., Ltd of China built the world's largest AC production company in 2014.

The Zhundong coalfield is located in the Xinjiang area, and the content of alkali and alkaline earth metals (AAEM) in Zhundong coal is high due to the complex coal-forming process, and in particular the sodium content is far higher than 2 wt%.<sup>2</sup> Compared with the conventional feedstock coal (e.g., Taixi coal and Datong coal), the high content of AAEM of Zhundong coal has a positive role in promoting pore development of AC, whereas the volatilization and release of AAEM from the coal may cause slagging and corrosion of the production equipment, which could cause safety problems for AC production.3

Currently, considerable amounts of research have focused on the release behavior of AAEM during coal combustion and gasification, and these studies revealed that a high temperature could induce strong volatilization of AAEM from coal.4,5 Thus, the temperature is thought of as the most important factor affecting the release behavior of AAEM from the coal.6 However, the temperature for coal-based AC preparation is lower than that of coal combustion and gasification, therefore, the amount of AAEM released by volatilization is less, meaning that any potential harm to the equipment would be much easier to control.1 Some researchers claimed that only a small amount of AAEM was released during Zhundong coal pyrolysis at high temperatures, and that the rest of the AAEM remained and enriched in the char.<sup>7,8</sup> By means of a great deal of work, some researchers proposed a concept of "carbon thermal reactions" between inorganics and the carbon matrix at high temperatures, which was attributed to the retention of AAEM in the coal char which had an influence on these reactions.9,10 Thus, it can

School of Chemical and Environmental Engineering, China University of Mining and Technology (Beijing), Beijing 100083, PR China. E-mail: liangdc@cumtb.edu.cn

#### Paper

be concluded that the presence of the carbon matrix has a significant inhibition on the release of AAEM in coal.<sup>2,11</sup> The previous results indicated that the consumption of the carbon matrix aggravated the volatilization and release of AAEM during Zhundong coal combustion and gasification. Because of this, the existence of a carbon matrix and a low temperature can effectively inhibit the volatilization and release of AAEM from the Zhundong coal in the preparation of AC.

Coal-based AC preparation consists of two stages: carbonization (pyrolysis) and activation (incomplete oxidation between the carbon matrix and  $H_2O/CO_2$ ), which is more complex than coal combustion or gasification.12 In addition, long-time pyrolysis and activation processes are beneficial to the complete development of the pore structure.13 However, the causal problem is that the longer the coal stays at a high temperature, the more AAEM would be released by volatilization from the coal.<sup>14</sup> At present, more attention has been given to the transformation of AAEM in Zhundong coal during the process of pyrolysis, combustion, and gasification, whereas less attention has been given to the AC preparation.7,15,16 In this case, it is necessary to reveal the transformation behavior of AAEM in the preparation of AC derived from Zhundong coal, which should be the pre-condition to evaluate systematically whether Zhundong coal could be used to prepare high-performance AC cleanly or not.

Accordingly, the main aim of this work was to investigate the transformation of AAEM in Zhundong coal during the preparation of AC. A typical Zhundong high-alkali coal was sampled and a series of investigations on the preparation of AC with different activation agents and temperatures were conducted. The char and AC samples produced were characterized to determine the content, chemical speciation, and distribution of AAEM. Then, the "FactSage" thermochemical software was employed to couple the pyrolysis and activation processes, and simulate the transformation of AAEM during the whole process. The goal of this work was to obtain a depth of understanding of the transformation of AAEM in the preparation process and to determine a feasible assessment of the preparation of AC from Zhundong coal.

### 2. Experimental

#### 2.1 Samples

A typical Zhundong high-alkali coal was ground in a mill until the particle size was less than 0.074 mm. These coal particles were pressed, at 200 MPa, into pellets with a thickness of 8 mm and a diameter of 25 mm, and then they were crushed into particles ranging from 3 mm to 10 mm. The char sample was prepared in a tube furnace by heating crushed coal briquettes from room-temperature to 600 °C with a heating rate of 5 °C min<sup>-1</sup> under an inert atmosphere of N<sub>2</sub> (100 mL min<sup>-1</sup>), and the holding time was 60 min. A previous study has demonstrated that the char obtained which had an amorphous structure and less graphite-like carbon was suitable for the subsequent activation process.<sup>1</sup> The coal and char samples were air-dried to a constant weight, and results of the proximate and ultimate analysis for the coal and char samples are summarized in Table 1.

Table 1 Analysis of the coal and ash samples

	Proximate analysis (wt%)				Ultimate analysis (wt%)				
Sample	M <sub>ad</sub>	Ad	V <sub>daf</sub>	FC <sub>daf</sub>	$C_{\mathrm{daf}}$	<i>H</i> daf	O <sub>daf</sub> (diff)	N <sub>daf</sub>	S <sub>t,d</sub>
Coal Char	10.13 4.50	4.17 6.22	30.93 16.11	69.07 83.89	70.54 84.83			0.69 0.60	0.77 0.63
<sup><i>a</i></sup> ad: air dried, d: dried, daf: dry ash-free, diff: by difference, t: total.									

The preparation of AC from the crushed coal briquettes is described in detail elsewhere.<sup>1</sup> In brief, the preparation of AC was more complex compared with that of the char, and the process was as follows: the crushed coal briquettes were heated to 600 °C under a N<sub>2</sub> atmosphere (100 mL min<sup>-1</sup>) with a holding time of 60 min, then steam (100 mL min<sup>-1</sup>) and CO<sub>2</sub> (100 mL min<sup>-1</sup>) were introduced into the tube furnace. Meanwhile, the reactor continued to heat up until the target temperature (700 °C, 800 °C, 850 °C, and 900 °C) was reached, and then was held for 2 h. The AC samples produced by this method were denoted as agent-temperature-AC, for example, CO<sub>2</sub>-800-AC was created with an activation temperature of 800 °C and the activation agent of AC was CO<sub>2</sub>.

#### 2.2 Characterization

Because of the pyrolysis and activation processes that had been experienced during the preparation of the AC samples, and the chemical properties of the carbon matrix in the AC, the samples are relatively stable. The traditional method for the determination of AAEM content in coal was to analyze the digested coal by ICP-OES.<sup>17</sup> However, the AC sample needed to be treated several times to be digested completely, and because of this it was easy to introduce errors into the process. The AC samples were converted to ash by gentle combustion at 500 °C and it was difficult to release the AAEM from the samples under this temperature. Therefore, it could simply be considered that the content of AAEM in the resulting ash was the same as that in the AC, and the composition of the ash was characterized by X-ray fluorescence spectrometry (XRF, ThermoFisher Scientific, ARL PERFORM'X 4200).

The surface chemistry of the samples was determined using X-ray photoelectron spectroscopy (XPS, ThermoFisher Scientific, ESCALAB 250Xi), and the apparatus was equipped with monochromatic Al-Ka X-rays, and the pass energy was 100 eV.

An evaluation of the morphologies of the previously mentioned samples and regional composition analysis was conducted using environmental scanning electron microscopy (ESEM, ThermoFisher Scientific, Quattro C), which was equipped with X-ray energy dispersive spectroscopy (EDS, AMETEK, Element E1868).

The Raman spectra of the AC samples were recorded with a confocal micro-Raman spectrometer (Renishaw, inVia), and the excitation laser beam with a 532 nm wavelength was focused on the sample by a microscope, then the Raman signal was collected in the direction of the backscattering. The Raman spectra in the range between 800 and  $1800 \text{ cm}^{-1}$  were collected and all the scans were performed three times, and the power of the laser focused on the sample surface was controlled at about 1 mW.

The chemical compositions of the char and AC samples were identified by X-ray diffraction (XRD, Malvern PANalytical, X'Pert<sup>3</sup> Powder) with Cu K $\alpha$  radiation. The qualitative powder XRD analysis was performed with an accelerating voltage and current of 40 kV and 40 mA, respectively. The XRD spectra were obtained between 5° and 85° with a step of 0.083° s<sup>-1</sup>.

#### 2.3 FactSage modelling

The thermodynamic equilibrium calculations, based on the principle of minimisation of the Gibbs free energy, were performed using FactSage (version 7.3) software.<sup>18,19</sup> FactSage with FToxide and FactPS was used to simulate the evolutionary behaviours of the AAEM species during the preparation of AC under different conditions as described in this paper. The calculated system was elaborately defined based on the XRF analyses of ash, and the required data for the thermodynamic

equilibrium calculations included: Al, C, Ca, Cl, H, K, Mg, N, Na, O, S, and Si.

## 3. Results and discussion

#### 3.1 Migration of AAEM during the preparation of AC

By investigating the variation of the AAEM contents in the pyrolysis and activation processes of Zhundong coal, the transformation of AAEM during the preparation of AC was deduced. The AAEM contents in raw coal, char, and AC samples with  $H_2O/CO_2$  at different temperatures are shown in Fig. 1.

Compared with the raw coal, the contents of Na and K in the AC decreased, whereas that of Mg and Ca increased. In particular, it can be observed from Fig. 1(a) that the decrease of Na content mainly occurred in the pyrolysis process, whereas the decline of the Na content tended to be stable as the temperature increased in the activation process, and the loss of Na content in the AC prepared with  $CO_2$  activation was less than that with  $H_2O$  activation. Fig. 1(b) shows that the variation of K content was similar to that of Na, but slightly different, in that the loss of K during  $H_2O$  activation was greater than that in pyrolysis. In

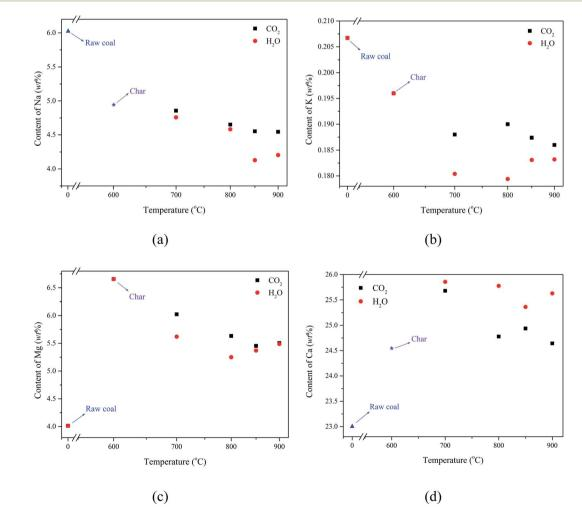


Fig. 1 The variation of AAEM content during the preparation of AC with H<sub>2</sub>O/CO<sub>2</sub> activation at different temperatures, (a) Na, (b) K, (c) Mg, and (d) Ca.

#### Paper

Fig. 1(c), the content of Mg increased greatly in the pyrolysis, and then the Mg content decreased slightly with the increase of temperature in the activation. Similar to Na and K, the loss of Mg content in  $CO_2$  activation was also less than that in  $H_2O$ activation. Finally, the change of Ca content was different from that of K, Mg, and Na, during the preparation of AC. The Ca species were enriched in both the char and AC, and the content of Ca in the AC prepared by  $H_2O$  activation was higher than that by  $CO_2$  activation, as shown in Fig. 1(d).

In order to explain the variation of the AAEM content, more advanced analytical methods were needed to explore the transformation of AAEM during the preparation of AC from Zhundong coal. The variation of the AAEM species on the surface of the AC before and after preparation was characterized by XPS. The XPS spectra of Na 1s, K 2p, Mg 1s, and Ca 2p are shown in Fig. 2.

From Fig. 2, the signal intensities of Ca, K, Mg, and Na, on the surface of the raw coal were weak, which indicated that the content of these AAEM species distributed on the surface of the coal was very low. After the pyrolysis of the coal, the signal intensities of Ca, K, Mg, and Na, on the surface of the obtained char increased greatly. This occurrence proved the fact that the AAEM species migrated from the interior of the coal matrix to the surface of the obtained char during coal pyrolysis, and it was identical with the results of previous research.<sup>7</sup> When the AC samples were derived from the char by  $CO_2$  or  $H_2O$  activation at different temperatures, the signal intensity of AAEM on the

surface of the AC samples was different from that of the char, but the differences were not obvious. From these differences, it was found that the change of AAEM signal intensity was consistent with the variation of AAEM content during the H<sub>2</sub>O or CO<sub>2</sub> activation at different temperatures. It was further inferred from the change of the AAEM signal intensity on the surface of AC that the decrease of K, Mg and Na, contents was because of the release of these species from the surface of the AC. Compared with the continuous decline of K and Na contents, the content of Mg increased in the pyrolysis whereas the Ca content was enriched in the whole process of the preparation of AC. The main reason for this was that Mg and Ca combined with carbon matrix through a double bond, which was stronger than the single bonds of K, and Na and the volatilization of the Ca and Mg species was weaker, and this led to Mg and Ca enrichment on the surface of AC. It was clear that these AAEM species migrated from the interior of the coal matrix to the surface, and were then volatilized from the surface of the char and AC. Therefore, it was necessary to investigate the distribution of AAEM species on the surface of the char and AC samples. The ESEM-EDS analysis was used to observe the change of microstructure and to explore the distribution of AAEM species on the surface during the preparation of AC. Some typical surface images and the results of the EDS analysis are shown in Fig. 3.

Elemental mapping is a powerful technique for observing the element distribution on the surface of the sample, and the

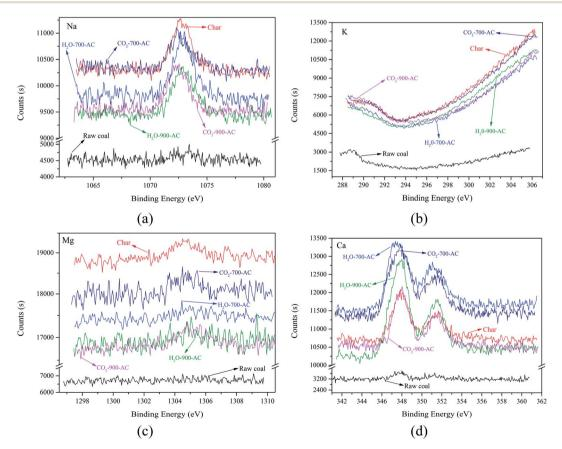
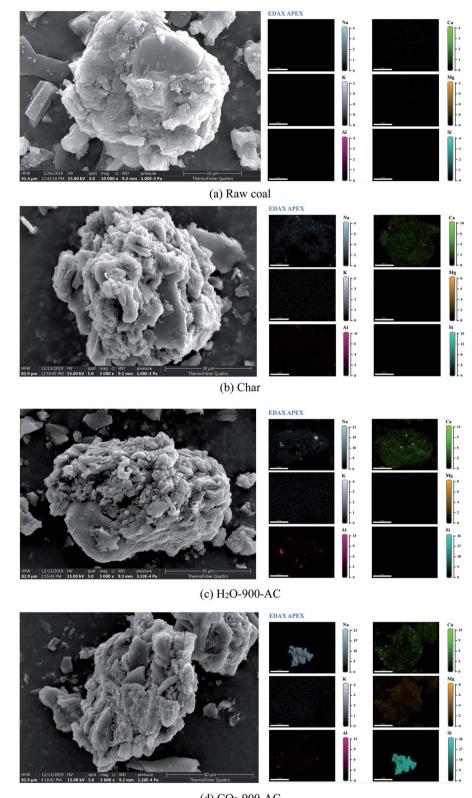


Fig. 2 High-resolution XPS spectra of the raw coal, char, and AC samples. (a) Na 1s, (b) K 2p, (c) Mg 1s and (d) Ca 2p.



(d) CO2-900-AC

Fig. 3 Scanning electron microscopy with energy dispersive X-ray analyses of the (a) raw coal, (b) char and (c) and (d) AC samples.

transformation of AAEM elements during the preparation of AC could be explored by using this technique. From the ESEM-EDS results shown in Fig. 3(a), it was observed that there were few

inorganic elements on the surface of the raw coal, and those were Al, Ca, K, Mg, Na, and Si. After the pyrolysis of the raw coal, the amount of Al, Ca, Mg, Na, and Si on the surface of the

#### Paper

obtained char was greatly increased, as shown in Fig. 3(b). It can be seen from Fig. 3(c) and (d) that these elements, Al, Ca, Mg, Na, and Si, were accumulated on the surface of the AC when the obtained char was further activated by  $H_2O$  or  $CO_2$ . In particular, the distribution of Na and Si on the surface of AC coincided when the AC was prepared by  $CO_2$  activation. This indicated that there was a large amount of Na bound to Si on the surface of AC, in addition to a small amount of Na volatilization during the preparation of the AC. Compared with  $CO_2$  activation, the difference in the preparation of AC by  $H_2O$  activation was that the distribution of Al, Na, and Si elements was similar, which suggested that these elements might be combined together. The transformation of the chemical speciation of these elements, especially Al, Na, and Si, in the process of AC preparation will be discussed in depth next.

# 3.2 Evolution of the microstructure during the preparation of AC

Using the analyses described previously, the transformation behavior of the AAEM was revealed during the preparation of AC derived from Zhundong coal. However, the causes of these phenomena were inferred from the evolution of the microstructure of the coal during the preparation process. According to the results of previous work,  $I_D/I_G$  was used as a significant parameter to investigate the graphite-like carbon or crystalline structure, and the  $I_D/I_G$  value of the char was 0.95, which was higher than that of the raw coal which was 0.62.1 This suggested that the defects and amorphous structure of the char increased when compared with the raw coal, during the pyrolysis.<sup>20</sup> The disordered surface morphology of the char was observed by ESEM and the results are shown in Fig. 3(b), which confirmed the  $I_{\rm D}/I_{\rm G}$  value result. Zhundong coal is a type of long flame coal, which is a characteristic of low grade bituminous coal. Based on these results, it was deduced that a large amount of volatile matter was released and it promoted the AAEM species inside the coal matrix to move towards the surface during the coal pyrolysis, moreover, the amorphous structure would help these AAEM species to migrate to the surface. As a result, there were a lot of AAEM species on the surface of the char, and then some

K and Na species were released from the surface because of their volatile properties. The microstructure evolution of the char during the activation process was also explored by Raman spectroscopy, and the Raman spectra with corrected baseline for the char and AC samples in the range of 800 to 1800 cm<sup>-1</sup>, are shown in Fig. 4(a). The GRAMS/32 AI software was used to deconvolute the Raman spectra into 10 Gaussian bands,<sup>21,22</sup> and the assignments of these bands represented specific structures, which had been recorded in previous work,<sup>23</sup> and the variations of  $I_D/I_G$  under different activation conditions are shown in Fig. 4(b).

Fig. 4(b) shows that the value of  $I_D/I_G$  increased with the increase of the temperature during the activation process, and it suggested that the defects and amorphous structure in AC increased whereas the graphite structure decreased in the process. Furthermore, the  $I_D/I_G$  values of the AC produced with H<sub>2</sub>O activation were higher than those of the AC produced with CO<sub>2</sub> activation. This also indicated that the defects and amorphous structure in the AC produced with H<sub>2</sub>O activation were more than those produced with H<sub>2</sub>O activation were more than those produced with CO<sub>2</sub> activation. This might explain why the content of K, Mg, and Na in the AC prepared with H<sub>2</sub>O activation was lower than that with CO<sub>2</sub> activation (Fig. 1). Because there were more disordered structures in the AC prepared with H<sub>2</sub>O activation, more K, Mg, and Na, species were directly exposed to a high temperature, which made these element species easier to volatilize and release from the AC.<sup>24</sup>

By studying the relationship between the structural evolution of AC and the transformation of AAEM, it could be concluded that the formation of defects and a disordered structure was beneficial to the generation of pores in the AC, which causes the AAEM species in the carbon matrix to be exposed to a high temperature environment, and this increased the probability of these AAEM volatilizations and release from the AC.

# 3.3 Transformation of AAEM chemical speciation during the preparation of AC

The XRD was performed to determine the chemical speciation of AAEM species in the raw coal, char and AC samples, and the

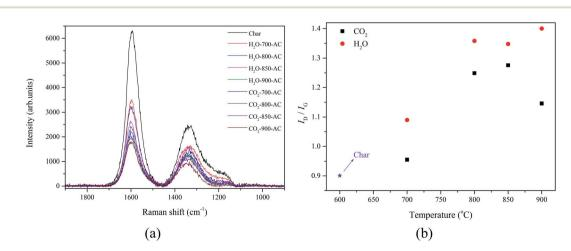


Fig. 4 Raman spectra of the char and AC samples (a) and  $I_D/I_G$  (b).

peak intensity for each mineral was characterised to indirectly show the content of each mineral phase in the samples.<sup>17</sup> The variation in some of the crystalline phases identified by XRD in these samples are shown in Fig. 5, and the information given next could be obtained from the XRD spectra. In the pyrolysis process, the peak intensity of SiO<sub>2</sub> decreased considerably. The CaSO<sub>4</sub>·2H<sub>2</sub>O signal disappeared whereas the CaSO<sub>4</sub> signal appeared in the char, and this indicated that most of the CaSO<sub>4</sub>·2H<sub>2</sub>O became CaSO<sub>4</sub> after dehydration. Additionally, there was some FeS in the raw coal, and then this FeS gradually changed into FeS<sub>2</sub> during the pyrolysis. When H<sub>2</sub>O was used to activate the char to prepare the AC, the peak intensity of SiO<sub>2</sub> decreased and finally disappeared as the activation temperature was increased. Based on the previous discussion, some of the SiO<sub>2</sub> that disappeared would react with the AAEM species to form AAEM silicate or aluminosilicate. This was confirmed by the ESEM-EDS characterization results, as shown in Fig. 3(d). Furthermore, the peak of Na<sub>2</sub>Al<sub>2</sub>SiO<sub>6</sub> was observed in H<sub>2</sub>O-700-AC, whereas these silicates and aluminosilicate were not detected by XRD in H<sub>2</sub>O-800-AC and H<sub>2</sub>O-800-AC. The probable reason for this occurrence was that these crystalline state substances were converted into the amorphous state at high temperatures, and the amorphous state substance cannot be detected by XRD.8 It could be found from Fig. 4 that the diffraction peaks of CaSO4 disappeared, whereas that of CaS

appeared in the AC. Previous research has demonstrated that the CaSO<sub>4</sub> reacted with the coal matrix at high temperatures to form CaS. This resulted in a decrease of the CaSO<sub>4</sub> content and the increase of CaS content during the preparation of AC. The transformation of minerals during the preparation of AC with CO<sub>2</sub> activation was consistent with that seen with the H<sub>2</sub>O activation. The difference was that the diffraction peak of CaCO<sub>3</sub> was observed in CO<sub>2</sub>-700-AC, and due to the existence of a large amount of CO<sub>2</sub>, some Ca species combined with CO<sub>2</sub> to form CaCO<sub>3</sub> at high temperatures.

However, it is important to realize that some information about amorphous materials and poorly crystalline materials cannot be detected using XRD, thus, there was little information about the transformation of AAEM chemical speciation during the preparation of AC only by using XRD. In order to make up for the shortcomings of the XRD characterization, FactSage was used as a modelling tool to systematically elucidate the chemical speciation of AAEM species during the preparation of AC from Zhundong coal according to the results of thermodynamic calculations, and the simulation results which are shown in Fig. 6.

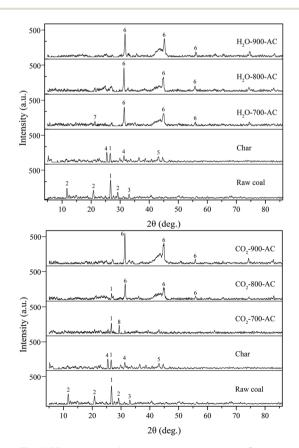


Fig. 5 The XRD patterns of the raw coal, char and AC samples. (1): SiO<sub>2</sub>, (2): CaSO<sub>4</sub>·2H<sub>2</sub>O, (3): FeS<sub>2</sub>, (4): CaSO<sub>4</sub>, (5): FeS, (6): CaS, (7): Na<sub>2</sub>Al<sub>2</sub>SiO<sub>6</sub>, (8): CaCO<sub>3</sub>.

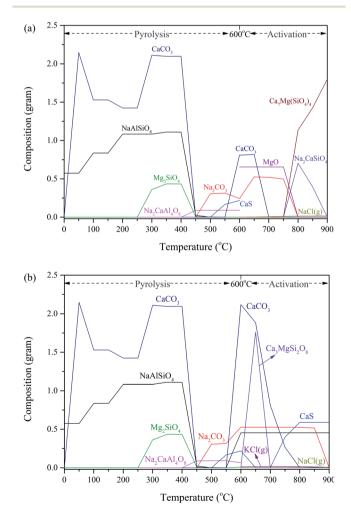


Fig. 6 Results from FactSage showing the evolution of the transformation behaviour of the AAEM species during the preparation of AC from Zhundong coal with (a)  $H_2O$  and (b)  $CO_2$  activation.

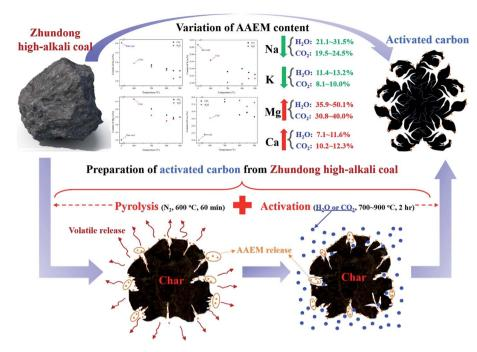


Fig. 7 Schematic of the behaviour of the AAEM transformation process during the preparation of AC from Zhundong high-alkali coal.

As Fig. 6 shows, the amount of NaCl and KCl in the gas phase produced by the coupling process of pyrolysis and CO<sub>2</sub> or H<sub>2</sub>O activation was very small. It is generally known that the generation of volatile AAEM species during high-alkali coal combustion or gasification leads to a large loss of their content, and then these volatilized AAEM species can cause damage to the production equipment and also pose potential risks to the safety of the production. Therefore, this situation can be avoided in the process of preparing AC from the Zhundong coal. Very few volatile AAEM species were generated in the preparation process of AC from Zhundong coal, moreover, the low temperature, as well as the presence of the carbon matrix, meant that the amount of these AAEM species released from the coal was negligible. Furthermore, in the whole preparation process, especially with the increase of activation temperature, it could be clearly observed that the silicate of a single AAEM element transformed into the silicate of multiple AAEM elements, e.g., Mg<sub>2</sub>SiO<sub>4</sub> and NaAlSiO<sub>4</sub> were transformed into Ca<sub>7</sub>Mg(SiO<sub>4</sub>)<sub>4</sub> and Na<sub>2</sub>CaSiO<sub>4</sub>, respectively. This might suggest that the silicate with multiple AAEM elements was more stable at higher temperatures. Finally, there were some differences in the evolution of the chemical speciation of AAEM in AC prepared with H<sub>2</sub>O and CO<sub>2</sub> activation. Among them, the obvious distinction was the change of AAEM carbonate content, such as Na<sub>2</sub>CO<sub>3</sub> and CaCO<sub>3</sub>, and the generation of these carbonates in the AC prepared with CO<sub>2</sub> activation was more than that in the AC prepared with H<sub>2</sub>O activation, moreover, the decomposition of these carbonates was slower in the process of CO<sub>2</sub> activation. In addition, the change of CaS obtained using a thermodynamic calculation was consistent with that of the XRD analysis in the process of CO<sub>2</sub> activation.

In conclusion, the transformation behaviour of AAEM species during the preparation of AC from Zhundong coal is shown in Fig. 7. According to the previous discussion, a large amount of volatiles would be produced and released from the coal during the pyrolysis process, and these released volatiles prompted the AAEM species inside the carbon matrix to move towards the surface of the char, meanwhile, this process also made some AAEM species which were not closely knit with the carbon matrix leave the surface of the char. With the activation process going on, the activation agent, such as H<sub>2</sub>O or CO<sub>2</sub>, reacted with the carbon matrix in the char, and then some AAEM species inside the char would be exposed at the same time as the pore formation occurred. Due to the reaction between some of the carbon matrix and the activation agent, the fixation effect of this carbon matrix on AAEM species would disappear, and then these AAEM species were released from the char. By means of XRD characterization and thermodynamic calculation, it was confirmed that the amount of AAEM with strong volatility and corrosiveness, such as NaCl and KCl, was very little in the whole process. Therefore, the preparation of AC from Zhundong coal can effectively inhibit the production and release of some harmful AAEM species.

### 4. Conclusion

During the preparation of AC from Zhundong high-alkali coal, the AAEM species inside the carbon matrix moved towards the surface of the AC. In this process, some Na and K species were released due to the weak binding with the carbon matrix, resulting in the loss of K and Na content. Compared with K and Na, Ca and Mg were closely combined with the carbon matrix, and they were enriched in the AC, which made the content of Mg and Ca increase. In addition, the defects and amorphous structure of the AC prepared with  $H_2O$  activation were more than those of the AC prepared with  $CO_2$ , which meant that more AAEM species were exposed to the high temperature environment. As a result, the loss of AAEM content in the AC with  $H_2O$  activation was higher than that in the AC with  $CO_2$  activation. In the whole process of AC preparation, the amount of AAEM species generated with strong volatility and corrosivity was very small, and the loss of AAEM content was mainly due to the release of volatile matter and the consumption of the carbon matrix. Therefore, the preparation of AC from Zhundong high-alkali coal is an effective route for its clean use.

## Conflicts of interest

There are no conflicts to declare.

## Acknowledgements

The authors gratefully acknowledge the financial support provided by the National Natural Science Foundation of China (Grant No. 22008255) and the Fundamental Research Funds for the Central Universities (Grant No. 2020XJHH01).

## References

- 1 D. Liang, Q. Xie, J. Liu, *et al.*, Mechanism of the evolution of pore structure during the preparation of activated carbon from Zhundong high-alkali coal based on gas-solid diffusion and activation reactions, *RSC Adv.*, 2020, **10**(55), 33566–33575.
- 2 R. Li, Q. Chen and H. Zhang, Detailed Investigation on Sodium (Na) Species Release and Transformation Mechanism during Pyrolysis and Char Gasification of High-Na Zhundong Coal, *Energy Fuels*, 2017, **31**(6), 5902– 5912.
- 3 L. Ding, Y. GAO, X. LI, *et al.*, A novel CO<sub>2</sub>-water leaching method for AAEM removal from Zhundong coal, *Fuel*, 2019, 237, 786–792.
- 4 C. Wang, L. Zhao, T. Han, *et al.*, Release and Transformation Behaviors of Sodium, Calcium, and Iron during Oxy-fuel Combustion of Zhundong Coals, *Energy Fuels*, 2018, **32**(2), 1242–1254.
- 5 Y. Liu, L. Cheng, Y. Zhao, *et al.*, Transformation behavior of alkali metals in high-alkali coals, *Fuel Process. Technol.*, 2018, **169**, 288–294.
- 6 X. Wang, Z. Xu, B. Wei, *et al.*, The ash deposition mechanism in boilers burning Zhundong coal with high contents of sodium and calcium: a study from ash evaporating to condensing, *Appl. Therm. Eng.*, 2015, **80**, 150–159.
- 7 D. Liang, Q. Xie, Z. Wei, *et al.*, Transformation of alkali and alkaline earth metals in Zhundong coal during pyrolysis in an entrained flow bed reactor, *J. Anal. Appl. Pyrolysis*, 2019, **142**, 104661.
- 8 Z. Ma, J. Bai, W. Li, *et al.*, Mineral Transformation in Char and Its Effect on Coal Char Gasification Reactivity at High

Temperatures, Part 1: Mineral Transformation in Char, *Energy Fuels*, 2013, 27(8), 4545–4554.

- 9 H. Zhang, J. Bai, L. Kong, *et al.*, Behavior of Minerals in Typical Shanxi Coking Coal during Pyrolysis, *Energy Fuels*, 2015, **29**(11), 6912–6919.
- 10 Z. Ma, J. Bai, X. Wen, *et al.*, Mineral Transformation in Char and Its Effect on Coal Char Gasification Reactivity at High Temperatures Part 3: Carbon Thermal Reaction, *Energy Fuels*, 2014, 28(5), 3066–3073.
- 11 Y. Zhao, D. Feng, Y. Zhang, *et al.*, Effect of pyrolysis temperature on char structure and chemical speciation of alkali and alkaline earth metallic species in biochar, *Fuel Process. Technol.*, 2016, **141**, 54–60.
- 12 M. A. Lillo-Rodenas, J. P. Marco-Lozar, D. Cazorla-Amoros, *et al.*, Activated carbons prepared by pyrolysis of mixtures of carbon precursor/alkaline hydroxide, *J. Anal. Appl. Pyrolysis*, 2007, **80**(1), 166–174.
- 13 Q. Xie, X. Zhang, L. Li, *et al.*, Porosity adjustment of activated carbon: theory, approaches and practice, *New Carbon Mater.*, 2005, **2**, 183–190.
- 14 C. Wang, X. Jin, Y. Wang, *et al.*, Release and Transformation of Sodium during Pyrolysis of Zhundong Coals, *Energy Fuels*, 2015, 29(1), 78–85.
- 15 H. Zhang, X. Guo and Z. Zhu, Effect of temperature on gasification performance and sodium transformation of Zhundong coal, *Fuel*, 2017, **189**, 301–311.
- 16 W. Li, L. Wang, Y. Qiao, *et al.*, Effect of atmosphere on the release behavior of alkali and alkaline earth metals during coal oxy-fuel combustion, *Fuel*, 2015, **139**, 164–170.
- 17 D. Liang, Q. Xie, H. Zhou, *et al.*, Catalytic effect of alkali and alkaline earth metals in different occurrence modes in Zhundong coals, *Asia-Pac. J. Chem. Eng.*, 2018, **13**(3), 1–13.
- 18 Y. Zhang, Q. Ren, H. Deng, *et al.*, Ash Fusion Properties and Mineral Transformation Behavior of Gasified Semichar at High Temperature under Oxidizing Atmosphere, *Energy Fuels*, 2017, **31**(12), 14228–14236.
- 19 Y. Yang, X. Lin, X. Chen, *et al.*, The formation of deposits and their evolutionary characteristics during pressurized gasification of Zhundong coal char, *Fuel*, 2018, 224, 469–480.
- 20 X. Li, J. Hayashi and C. Li, FT-Raman spectroscopic study of the evolution of char structure during the pyrolysis of a Victorian brown coal, *Fuel*, 2006, **85**(12–13), 1700–1707.
- 21 L. Zhang, T. Li, S. Wang, *et al.*, Changes in char structure during the thermal treatment of nascent chars in N<sub>2</sub> and subsequent gasification in O<sub>2</sub>, *Fuel*, 2017, **199**, 264–271.
- 22 W. Guo, Y. Wang, X. Lin, *et al.*, Structure and CO<sub>2</sub> gasification reactivity of char derived through pressured hydropyrolysis from low-rank coal, *Energy Fuels*, 2019, 33(9), 8032–8039.
- 23 D. Liang, Q. Xie, C. Wan, *et al.*, Evolution of structural and surface chemistry during pyrolysis of Zhundong coal in an entrained-flow bed reactor, *J. Anal. Appl. Pyrolysis*, 2019, **140**, 331–338.
- 24 Y. Bai, P. Lv, X. Yang, *et al.*, Gasification of coal char in  $H_2O/CO_2$  atmospheres: Evolution of surface morphology and pore structure, *Fuel*, 2018, **218**, 236–246.